Evolution of Mixing Regions in Jet and Swirling Jet in Crossflow: An Experimental Study

Theewara Yingjaroen,[1] Alongkorn Pimpin,[2] and Asi Bunyajitradulya[3*]

[1,2,3] Department of Mechanical Engineering, Faculty of Engineering, Chulalongkorn University
Bangkok 10330, Thailand
Tel: 02-218-6645, Fax: 02-252-2889
Email: thevara14@yahoo.com,[1] Alongkorn.P@eng.chula.ac.th,[2] Asi.B@chula.ac.th[3*]

Abstract

Evolution of mixing characteristics of jet in crossflow (JICF) and swirling jet in crossflow (SJICF) with non-zero tangential velocity is experimentally investigated. The diagnostic technique is the imaging of the extinction phenomena in conjunction with passive and reactive scalars techniques. From the traverse profiles, JICF mixing can be described approximately as from the outer region of the reactive profile, and the evolution of JICF mixing as progressing inward. There are three mixing regions. It evolves from passive outer-region mixing dominate in the very near field to central-region mixing dominate further downstream. Reactive inner-region mixing is, and remains, relatively small. For SJICF with swirl ratio of 0.5, there are practically only two mixing regions, inner and outer, throughout the flow evolution, and both occurs early upstream. The outer region mixing is relatively more intense, nonetheless. For swirl ratio 0.8, the mixing characteristic evolves from that similar to swirl ratio 0.5 to that similar to JICF. Therefore, the results of the two swirl ratios show that swirl causes inner region mixing in the near field. Finally, for SJICF the spanwise profiles show both the reactive and passive peaks to locate on the suction side, while mixing is found to be more effective towards the pressure side of the peaks.

Keywords: evolution, mixing, mixing regions, jet in crossflow, swirling jet in crossflow.

1. Introduction

This study describes our preliminary results from the continued effort in the study of jet in crossflow (JICF) and swirling jet in crossflow (SJICF) with non-zero tangential velocity, [1-3]. The present investigation attempts to explore two aspects. One is the evolution of mixing characteristics of these jets. In this respect, past works have made considerable progress towards the understanding of the mixing of JICF, [4-11]. Nonetheless, with the use of both reactive and passive scalar techniques, the present work attempts to bring forth further aspects of the mixing of these flows. In addition, fewer works have addressed the mixing of SJICF [12-15], especially in the non-zero tangential velocity configuration. The other aspect is related to an issue arisen from our past studies; namely, the effect of the initial swirl, or azimuthal, velocity profile on the characteristics of SJICF, [1-3]. Specifically, our past works have shown the location of maximum temperature to be located on the suction side. In the present work, we further attempt to explore similar aspect for scalars. It should be noted early on that the present work is in different flow regime from our past works. Specifically, the jet Reynolds number in the present work is much lower and is in the laminar flow range.

2. Experiment and Experimental Techniques

Experiments are conducted in a 20×20 cm^2 upwardly overflow, vertical water channel made from acrylic plates. Flow conditioning of the crossflow before it enters the test section includes, from upstream to downstream, two screens, plastic-straw honeycomb with one screen covered at each end, and another four screens. The swirling jet setup is an 8-mm rotating acrylic tube with honeycomb, driven by a motor-pulley system. The flow conditioning, from upstream to downstream, includes one screen, plastic-straw honeycomb with one screen covered at each end, and another three screens. There are five plastic straws in the honeycomb, whose nominal length-to-diameter ratio is 35. The last screen is located at 8.4 diameters upstream of the jet exit. The jet setup is gravity-fed with overflow tank.

In this investigation, flow visualization technique based on extinction phenomena and Beer's law is employed (see, e.g., [16]) in conjunction with both passive and reactive scalar techniques. In both techniques, an alkaline jet (NaOH solution) seeded with phenolphthalein is used, hence magenta in color. For the passive scalar technique, the crossflow fluid is plain water. For the reactive scalars technique, the crossflow fluid is acidic (HNO_3 solution), resulting in acid-base reaction when the alkaline jet entrains and mixes with the acidic crossflow and which turns the mixture into clear color after the predetermined stoichiometric ratio is reached. Hence, the magenta-colored region in the passive scalar technique marks the region of jet fluid,

while that in the reactive scalars technique marks only the region of the jet fluid which has not yet mixed with the crossflow fluid to the stoichiometric ratio. It can be inferred that the difference between the marked regions from the two techniques approximates the region in which the jet fluid has mixed with the crossflow fluid, at least upto the predetermined stoichiometric ratio.

The experiments are conducted at jet-to-crossflow effective velocity ratio (r) of 3.8, jet Reynolds number of 1,300, and swirl ratios (Sr) of 0 (JICF), 0.5, and 0.8. Mixing is investigated at volumetric stoichiometric ratio crossflow-to-jet of 1.3:1. Note that the stoichiometric ratio is determined by direct titration of the jet and crossflow fluids from the reservoirs before and after each run. The uncertainty for r is estimated to be ± 0.5, for Sr (except at 0) to be ± 0.1, and for stoichiometric ratio to be ± 0.1. Note that all velocities are averaged velocities, determined from measured flowrate and flow area. No detailed measurements of velocity distributions have been performed. For convenience, we shall refer to these different swirl cases as Sr0 (JICF), Sr05 (Sr = 0.5), and Sr08 (Sr = 0.8). In the case of SJICF, we shall denote the suction side (the lateral side at which the azimuthal velocity of the jet is in the same direction as the velocity of the cross flow) as S, and the pressure side (the opposite side) as P.

In imaging, the flow is backlight-illuminated with household fluorescence lambs through a semi-transparent white acrylic plate and is imaged onto a CCD video camera. The sequences of images are then extracted, and the mean extinction signal is calculated from the green signal according to

$$\overline{C_N}_{ij} = -\frac{1}{n}\sum_{k=1}^{n} \ln\left[(X_{ij,k} - \overline{NR}_{ij})/(\overline{B}_{ij} - \overline{NR}_{ij}\right],$$

where X is the image with the jet on, B is the image with the jet off (i.e., backlight only) while $\overline{B}$ is the mean of a sequence of B, NR is dark-noise image of the camera while $\overline{NR}$ is the corresponding mean, ij is pixel indices, and k is image index. In this experiment, the mean is calculated from the total of n = 3,000 images. Note that due to the technique, the mean signal $\overline{C_N}$ is already an integrated signal along the line of sight and is approximately proportional to the amount of the scalar at that location. No direct calibration to relate the physical amount of the scalar to the signal has been performed, however. The right-handed coordinates system employed in presenting the results is the followings: x is streamwise, y is wall normal, z is spanwise, and the origin is located at the center of the jet.

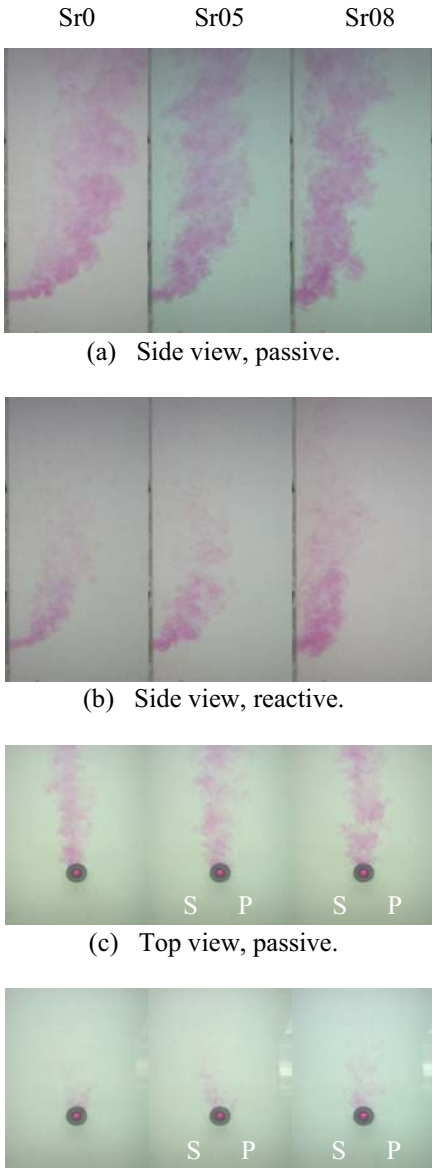

(a) Side view, passive.

(b) Side view, reactive.

(c) Top view, passive.

(d) Top view, reactive.

Fig. 1. Instantaneous images.

3. Results and Discussion

Figure 1 shows examples of instantaneous images from both side and top views, and both passive and reactive cases. Large-scale structures can be observed in both views. In the passive case, there is no reaction and the marked fluid persists to the end of view. In contrast, due to the reaction, the marked fluid in the reactive cases

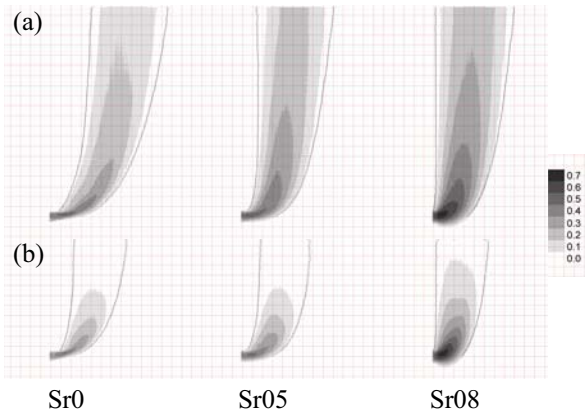

Fig. 2. Side View: Line-of-sight-integrated mean images, $\overline{C_N}$. (a) passive, (b) reactive.

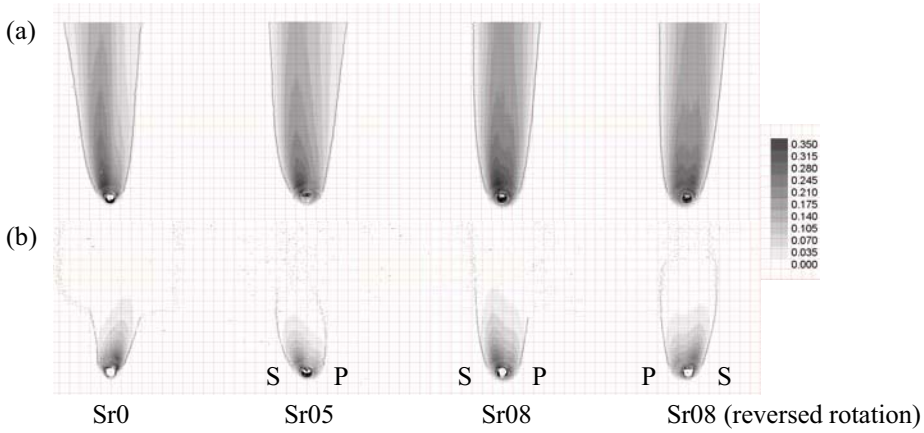

Fig. 3. Top View: Line-of-sight-integrated mean images, $\overline{C_N}$. (a) passive, (b) reactive.

gradually fades away in the downstream direction as the jet entrains and mixes with the surrounding crossflow. Of notable in the side views of both (a) and (b) is the reduction of jet penetration when swirl is increased.

Figure 2 shows the side view contours of the line-of-sight-integrated mean images, $\overline{C_N}$. As seen in the instantaneous images (Fig. 1), on the average JICF is observed to penetrate deeper into the crossflow; and, as swirl increases, the penetration depth decreases. Though not shown here, this also reflects in the jet trajectory, defined as the locus of the point of maximum $\overline{C_N}$ along the traverse. In general, the marked fluid is observed to be highly concentrated near the jet exit, and the contours of constant $\overline{C_N}$ are looped and deflected towards the crossflow. Note that in the reactive cases the region of marked fluid approximates the region of 'unburned fuel'. We shall postpone further detailed discussions regarding mixing to Figs. 4 and 5. Similarly, Fig. 3 shows the top view contours of the line-of-sight-integrated mean images, $\overline{C_N}$. The result shows some asymmetry, which is expectable (see [4]), but possibly some slight change in condition in the cases of JICF. For SJICF and for both passive and reactive cases, the maximum $\overline{C_N}$ is observed to locate on the suction side. In order to obtain some indications against some bias that may exist in the system and to further check the results, experiment with reversed rotational direction is performed in case of swirl ratio 0.8, and the result shows that the maximum still remains on the suction side.

JICF and SJICF Mixing

To gain better view of mixing, the traverse profiles of $\overline{C_N}$ at various downstream locations are plotted against the *rd*-normalized traversed coordinate in Fig. 4. Note that d is the diameter of the jet. For JICF, it is observed that the traverse location of the maximum $\overline{C_N}$ of the passive profile is always located further out from the wall than that of the reactive profile. In order to discuss the mixing, we use the traverse location of the corresponding maximum $\overline{C_N}$ as a reference point to differentiate the *outer region*, O , (away from the wall) from the *inner region*, I , (towards the wall). Thus, we divide the flow into two sets of regions: O_r and I_r , and O_p and I_p , which correspond to the outer and the inner regions of the reactive profile, or *reactive outer* and *inner regions*, and the outer and the inner regions of the passive profile, or *passive outer* and *inner regions*, respectively. The divisions are shown with two solid arrows as an example for JICF.

For JICF, the followings can be observed.

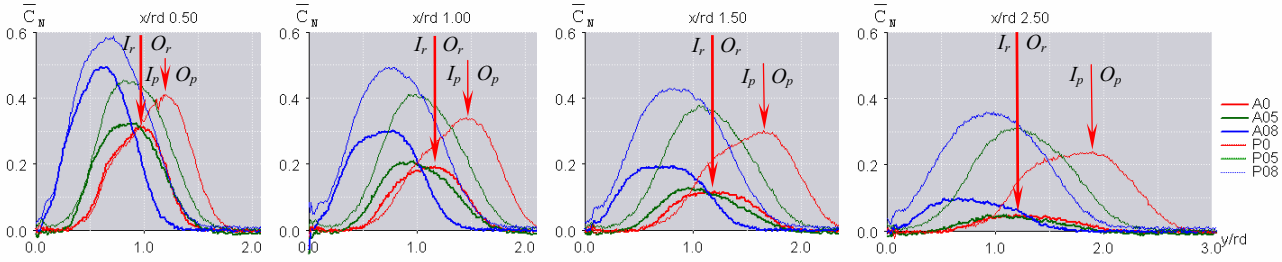

Fig. 4. Traverse profiles (side view) of $\overline{C_N}$ at various downstream locations. Legends: P denotes the passive cases (thinner line), A denotes the reactive cases (thicker line). The number indicates the level of swirl ratio.

1. In the very near field ($x/rd = 0.5$), the difference in areas under the passive and the reactive profiles lies mostly in the outer region of the passive profile, i.e., the O_p region.

   However, there is already some difference in areas in the inner region of the passive profile, from the location of the peak of the passive profile down to the location of the peak of the reactive profile. This is the overlap region between I_p and O_r, the region between the two arrows shown in the figure. Because this overlap region plays important role in mixing further downstream, we shall refer to it as the *central region*, C .
2. As the flow evolves further downstream from x/rd = 0.5 to 2.5, the difference in areas of the two profiles in the central region progressively becomes larger and the central region progressively becomes wider.

   On the other hand, the difference in areas in the O_p region stays relatively constant, especially beyond $x/rd >\sim 1.5$. Note that the difference in the O_p region beyond $x/rd >\sim 1.5$ is basically the area under the passive profile since $\overline{C_N}$ of the reactive profile virtually vanishes.
3. There is relatively little difference in areas of the two profiles in the inner region of the reactive profile, i.e., the I_r region. Nonetheless, some relatively small difference can be observed downstream, e.g., starting at $x/rd \approx 1.0$. Yet, the difference in this region remains relatively small as the flow evolves downstream.
4. The maximum $\overline{C_N}$ in the reactive profile is approximately located at the same traverse position as that of the inner edge of the central plateau in the passive profile.

   Thus, the traverse location and the span of the central region roughly corresponds to the traverse location and the span of the *plateau region* of the passive profile. Hence, from (1), as the flow evolves further downstream from x/rd = 0.5 to 2.5, the plateau region of the passive profile progressively becomes wider.

Before the results are discussed, the followings are noted. Firstly, due to the technique, $\overline{C_N}$ is already line-of-sight-integrated, e.g., in Fig. 4 it is the spanwise integration. Secondly, the area under the passive profile represents both 'burned' and 'unburned' jet fluid, while that under the reactive profile represents only the 'unburned' jet fluid, i.e., not yet mixed to the prescribed stoichiometric ratio. The difference of the two areas then represents the 'consumed, or burned, jet fluid.' This 'consumed' amount is used to indicate mixing in the region of interest.

With these, mixing in JICF can be described as follows. (1) In the very near field ($x/rd <\sim 0.5$), most of the mixing occurs in the outer region of the passive profile, i.e., the O_p region. However, there are already some mixing in the inner region of the passive profile, from the location of the peak of the passive profile down to the location of the peak of the reactive profile, i.e., the central region. (2) As the flow evolves further downstream from $x/rd = 0.5$, mixing occurs progressively more in the central region and the central region becomes wider. On the other hand, beyond $x/rd >\sim 1.5$ mixing in the O_p region becomes progressively less since the region has run out of 'unburned' fuel. (3) There is relatively little mixing in the inner region of the reactive profile, i.e., the I_r region. Nonetheless, some relatively small mixing can be observed downstream, e.g., starting at $x/rd \approx 1.0$. Yet, the mixing in this region remains relatively small as the flow evolves downstream.

In this respect, a simple view of the downstream evolution of JICF mixing can be constructed from the reactive and the passive profiles as follows. Consider the reactive profile as a 'pile of unburned fuel' and the passive profile above it (the difference of the two profiles) as the 'deposit of burned fuel.' We can see by looking from upstream to downstream that mixing of the 'unburned fuel' (the reactive profile) occurs mainly in the outer region of the reactive profile (O_r) and progresses inward (from outer to inner). Recall that the results are line-of-sight-integrated, hence mixing in the 'outer region' can have significant or large contribution from mixing at lateral sides.

From these, we divide the mixing of JICF into three regions.

- O_p -region mixing:

  This mixing occurs intensely and mainly in the near field. As the flow evolves downstream, it plays less important role since the region has run out of 'fuel.'

  The mixing in this region can be explained by the entrainment and mixing mechanism of the windward jet shear layer.

- Central-region mixing:

  This mixing starts in the near field and possibly as early as the O_p -region mixing. In the very near field, it is relatively less intense than the O_p -region mixing. However, as the flow evolves downstream, it phases in as the O_p -region mixing phases out, and it progressively becomes dominant. The reason is that there is still 'unburned' fuel in this region. Nonetheless, a mechanism is required to mix and burn this fuel.

  The mixing in this region is likely to predominantly associate with the entrainment and mixing mechanism of the hanging vortices and the developing CVP at the lateral sides of the jet.

- I_r -region mixing:

  The mixing in this region is relatively small and remains relatively small as the flow evolves downstream.

Using similar approach as that of JICF, the results of SJICF can be described as follows. From Fig. 4, for Sr05, the traverse locations of the reactive and passive peaks are at approximately the same position. Thus, (mixing in) the central region is negligible, and there are practically only the outer and the inner regions (mixing). The results show that mixing occurs both in the outer and inner regions, and both occurs early upstream in the near field. Nonetheless, in the upstream region the outer region mixing is relatively more intense. For Sr08, in the upstream region the traverse locations of the reactive and passive peaks are at approximately the same position, similar to Sr05. However, as the flow evolves further downstream, the two peaks shift off each other and the characteristic of the peaks becomes similar to JICF. Thus, in this case, the flow has two mixing regions upstream, but then evolves to have three mixing regions further downstream. The third region, i.e., the central region, emerges. Hence, in the upstream region, mixing characteristics of Sr08 is similar to Sr05, while further downstream it is similar to JICF. In this respect, the facts that the two peaks start to shift off each other and that the central-region mixing emerges suggest to a relatively more effective outer-region mixing mechanism or, e.g., a relative decay of the inner-region mixing mechanism. Finally, in comparison to JICF, it is seen that swirl causes inner region mixing in the near field.

Figure 5 shows similar plots for the spanwise profiles (top view). For JICF, comparing between the reactive and passive profiles at $x/rd = 0.5$, it can be noted that there is some slight change in the experimental condition of the flow. Nonetheless, observe that the widths of the jet, as indicated by the widths at the base, for both cases are more or less consistent. For SJICF, the figure shows the spanwise locations of the maximum for all cases (Sr05 or Sr08, and reactive or passive) to be on the suction side. For each swirl, the corresponding spanwise locations of the peaks of the reactive and passive profiles stay approximately at the same position. Furthermore, all profiles are skewed, with the peak locating on suction side and the tail pointing to the pressure side, at least upto the presented downstream location. (Note that the experimental data, not shown here, show that further downstream the passive profile of Sr08 becomes less skewed.) Mixing is observed more towards the pressure side of the peaks. This can be explained by larger shear on that side. Finally, for the reactive profiles, it is interesting to note the kink and the slight leveling off, resulting in a small plateau, near $z = 0$, see also Fig. 3. At this point, it is speculated that this is possibly related to low velocity, or recirculation, region of the flow.

4. Conclusion

The evolution of mixing characteristics of jet in crossflow (JICF) and swirling jet in crossflow (SJICF) with non-zero tangential velocity is experimentally investigated. The diagnostic technique is the imaging of the extinction phenomena in conjunction with passive and reactive scalars techniques.

Using the traverse locations of the maxima of the spanwise-integrated reactive and passive profiles as reference (for which the reference case JICF has its reactive peak located closer to the wall than its passive peak), mixing is divided into three regions: the passive outer region (O_p -region mixing), the central region, and the reactive inner region (I_r -region mixing).

For JICF, mixing can be described approximately as from the outer region of the reactive profile, and the evolution of JICF mixing as progressing inward (from outer to inner). There are three mixing regions. The results shows that early upstream there are both O_p -region and central-region mixings. However, the O_p -region mixing is relatively more intense for $x/rd < 0.5$. As the flow evolves further downstream, however, the O_p -region mixing phases out due to little 'unburned fuel' left in the region, while the central-region mixing phases in and plays more dominant role. Although there are some mixing in the reactive inner region, the I_r -region mixing is relatively small and remains relatively small as the flow evolves downstream, at least to the limit of the current experiment. The O_p -region mixing is attributed to relate predominantly to the entrainment and mixing mechanism of the windward jet shear layer; while the central region mixing to the hanging vortices and the

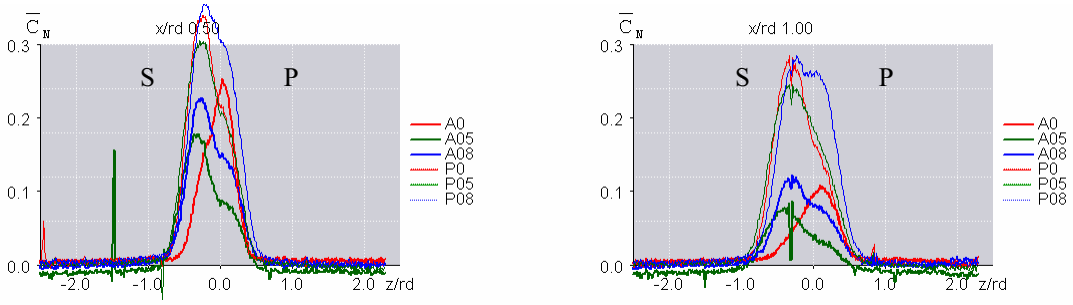

Fig. 5. Spanwise profiles (top view) of $\overline{C_N}$ at $x/rd = 0.5$ and 1.0.

developing CVP.

For SJICF Sr05, since the reactive and passive peaks stay correspondingly at approximately the same traverse position throughout the downstream extent investigated, its mixing characteristic can be described approximately by two mixing regions: the inner region and the outer region. The results show that mixing occurs both in the outer and inner regions, and both occurs early upstream in the near field. However, generally the outer region mixing is relatively more intense. For SJICF Sr08, in the upstream region the results show its mixing characteristic to be similar to Sr05 (i.e., traverse locations of the reactive and passive peaks coincide, and there are only outer and inner region mixings). Further downstream, however, it evolves to be similar to JICF (i.e., the two peaks start to shift off and the central-region mixing emerges as the third mixing region). The results of the two swirl ratios therefore show that swirl causes inner region mixing in the near field.

Finally, for SJICF the spanwise profiles show both the reactive and passive peaks to locate on the suction side, while mixing is found to be more effective towards the pressure side of the peaks.

References

[1] Wangjiraniran, W., and Bunyajitradulya, A., 2001. Temperature distribution in non-zero circulation swirling jet in crossflow. Proceedings of the Fifteenth Conference of The Mechanical Engineering Network of Thailand, Bangkok, Thailand, 28-30 November 2001, Vol. 1, pp. TF104-TF116.

[2] Sathapornnanon, S., and Bunyajitradulya, A., 2002. Effects of delta tab on temperature distribution in non-zero circulation swirling jet in crossflow. Proceedings of The Sixteenth Conference of The Mechanical Engineering Network of Thailand, Phuket, Thailand, 14-16 October 2002, pp. 72-77.

[3] Bunyajitradulya, A., and Sathapornnanon, S., 2005. Sensitivity to tab disturbance of the mean flow structure of nonswirling jet and swirling jet in crossflow. Phys. Fluids 17, CID 045102.

[4] Smith, S. H., and Mungal, M. G., 1998. Mixing, structure and scaling of the jet in crossflow. J. Fluid Mech., Vol. 357, pp. 83-122.

[5] Hasselbrink, E. F., Jr., and Mungal, M. G., 2001. Transverse jets and jet flames. Part 1. Scaling laws for strong transverse jets. J. Fluid Mech., Vol. 443, pp. 1-25.

[6] Hasselbrink, E. F., Jr., and Mungal, M. G., 2001. Transverse jets and jet flames. Part 2. Velocity and OH field imaging. J. Fluid Mech., Vol. 443, pp. 27-68.

[7] Su, L. K., and Mungal, M. G., 2004. Simultaneous measurements of scalar and velocity field evolution in turbulent crossflowing jets. J. Fluid Mech., Vol. 513, pp. 1-45.

[8] Yuan, L. L., and Street, R. L., 1998. Trajectory and entrainment of a round jet in crossflow. Phys. Fluids, Vol. 10, No. 9, pp. 2323-2335.

[9] Yuan, L. L., Street, R. L., and Ferziger, J. H., 1999. Large-eddy simulations of a round jet in crossflow. J. Fluid Mech., Vol. 379, pp. 71-104.

[10] Denev, J., Fröhlich, J., Bockhorn, H., 2005. Evaluation of mixing and chemical reactions within a jet in crossflow by means of LES. Proc. of European Combustion Meeting, Louvain, Belgium, 3.-6.4.2005.

[11] Muppidi, S., and Mahesh, K., 2006. Passive scalar mixing in jets in crossflow. AIAA-2006-1098, The 44th AIAA Aerospace Sciences Meeting and Exhibit, Reno, Nevada, Jan. 9-12, 2006.

[12] Kavsaoğlu, M. S., and Schetz, J. A., 1989. Effects of swirl and high turbulence on a jet in a crossflow. J. Aircr., Vol. 26, No. 6, pp. 539-546.

[13] Yoshizako, H., Yoshida, K., and Akiyama, I., 1991. Diffusion of a jet injected perpendicularly into uniform cross flow. Trans. Jpn. Soc. Mech. Eng., Ser. A, Vol. 57, pp. 354-359.

[14] Niederhaus, C. E., Champagne, F. H., and Jacobs, J. W., 1997. Scalar transport in a swirling transverse jet. AIAA J., Vol. 35, pp. 1697-1704.

[15] Denev, J. A., Fröhlich, J., and Bockhorn, H., 2005. Structure and mixing of a swirling transverse jet into a crossflow. In Humphrey et al. (eds.), Procs. of 4th Int. Symp. on Turbulent Shear Flow Phenomena, Williamsburg, June 27-29, 2005, pp. 1255-1260.

[16] Johari, H., and Paduano, R., 1997. Dilution and mixing in an unsteady jet. Exp. in Fluids, Vol. 23, pp. 272-290.